The role of scaffold architecture and composition on the bone formation by adipose derived stem cells

Heidi A. Declercq, PhD[1], Tim Desmet, MSc[2], Peter Dubruel, PhD[2], Maria J. Cornelissen, PhD[1*]

[1]Department of Basic Medical Sciences, Ghent University, De Pintelaan 185 6B3, Ghent, 9000, Belgium

[2]Polymer Chemistry & Biomaterials Research Group, Ghent University, Krijgslaan 281 S4 Bis, Ghent, 9000, Belgium

Keywords: three-dimensional plotting, poly-ε-caprolactone, surface modification, scaffold architecture, tissue engineering

Contact information:

heidi.declercq@ugent.be; Tel: +3293325133; Fax: +32093323823

ti.desmet@ugent.be; Tel: +3292644466; Fax: +3292644972

peter.dubruel@ugent.be; Tel: +3292644466; Fax: +3292644972

* ria.cornelissen@ugent.be; Tel: +3293325132; Fax: +32093323823

ABSTRACT

Scaffold architecture and composition are crucial parameters determining the initial cell spatial distribution and consequently bone tissue formation. Three-dimensional poly-ε-caprolactone (PCL) scaffolds with a 0/90 ° lay-down pattern were plotted and subjected to 1) an oxygen plasma (PCL O) or 2) a post-argon plasma modification with gelatin and fibronectin (PCL Fn). These scaffolds with an open pore structure were compared with more compact scaffolds fabricated by conventional processing techniques: oxidized polylactic acid (LA O) and collagen (COL) scaffolds. Human adipose tissue derived stem cell/scaffold interaction was studied.

The study revealed that the biomimetic surface modification of plotted scaffolds did not increase the seeding efficiency. The proliferation and colonization was superior for PCL Fn in comparison with PCL O. The plotted PCL Fn was completely colonized throughout the scaffold whereas conventional scaffolds only at the edge. Protein-based scaffolds (PCL Fn and COL) enhanced the differentiation, although plotted scaffolds showed a delay in their differentiation compared with compact scaffolds. In conclusion, protein modification of plotted PCL scaffolds enhances uniform tissue formation but shows a delayed differentiation in comparison with compact scaffolds. The present study demonstrates that biomimetic PCL scaffolds could serve as a guiding template to obtain a uniform bone tissue formation *in vivo*.

INTRODUCTION

Among the different tissue engineering (TE) strategies, the scaffold plays an important role as temporary support for the development of new tissue either through *in vivo* guiding cell growth in the scaffold or through *in vitro* culturing cells on the scaffold prior to implantation. In *in vivo* developmental processes, tissue formation is often preceded by high cell densities.[1] This important biological aspect has to be taken into account at the level of designing three-dimensional (3D) scaffolds for TE applications. During the last decades, many different processing techniques have been developed to design and fabricate 3D scaffolds resulting in an evolution from pre-formed scaffolds to patient-specific implants. These scaffolds, fabricated by diverse methods, have different physical architectures ranging from porous to fibrous and irregular to uniform. It is known that scaffold architecture plays a critical role in regulating cell spatial distribution, affecting the cellular signal expression and consequently tissue formation.[2-4] In scaffolds processed by conventional techniques (porogen leaching, gas foaming, solvent casting), cell migration and tissue ingrowth are often limited to the peripheral region resulting in a localized, non-uniform tissue formation.[2] In contrast, scaffolds fabricated by rapid prototyping (RP) techniques suffer from low resolution leading to scaffolds with large pore sizes, highly geometrical designs resulting in an open pore architecture with 100 % interconnectivity, influencing the tissue formation.[5] Poly-ε-caprolactone (PCL) and poly-lactic acid (LA) find wide application for the processing of scaffolds. Although PCL is a preferred polymer for RP techniques, a disadvantage is its intrinsic hydrophobicity and lack of functional groups resulting in poor cell attachment.[6] To enhance the bioactive properties of PCL, various surface modification techniques are reported.[7-19] Among these, plasma-based approaches have gained considerable popularity.[14-16,18,19] One of the major limitations of plasma technologies is the diversity of functional groups and the fact that the induced surface properties are not permanent.[18] More recently,

studies have been focusing on the use of plasma-treated surfaces as interfacial bonding layers for the subsequent immobilization of well-defined chemical species/molecules. Hence, achieving a more controlled surface chemistry which is designed to elicit specific biological responses can be reached.[18,20] Collagen has been among the most widely used biomaterials for biomedical applications.[21] However, due to some disadvantages, there is a shift towards surface modification of implants with collagen or gelatin.[8,22] Fibronectin (Fn), a glycoprotein, stimulates initial cell adhesion, but importantly, it should be immobilized in a biological active conformation. It was reported that Fn has an affinity for gelatin.[23] In our previous studies, we have shown that PCL films and scaffolds could be successfully modified using a multistep protocol, involving a plasma pretreatment, an UV-induced 2-amino-ethylmethacrylate (AEMA)-graft polymerization followed by the immobilization of gelatin and physisorbtion of Fn.[24-26]

The hypothesis of this study is that cell density is a crucial factor in the differentiation process and tissue formation in 3D scaffolds and can be regulated by the scaffold architecture and composition. The influence of scaffold architecture (plotted versus conventional scaffold) and composition/surface chemistry (oxidized polyester versus protein-based surfaces) on adipose tissue derived stem cell (ADSC) adhesion, proliferation, colonization and differentiation was studied. Two modification strategies, 1) an oxygen plasma modification and 2) a double protein coating via post-argon plasma AEMA grafting followed by gelatin immobilization and Fn physisorption, on plotted PCL scaffolds were compared. These plotted scaffolds with an open pore architecture were compared with conventional scaffolds based on oxidized poly D,D-L,L-lactic acid (LA O) and collagen (COL) having a more compact architecture with an irregular pore network.

MATERIALS AND METHODS

Three-dimensional PCL scaffold fabrication

Poly-ε-caprolactone (PCL) pellets (MW = 80 000 $g.mol^{-1}$) were obtained from Sigma-Aldrich Company. Porous cylindrical PCL scaffolds with a height of 3 mm and a diameter of 4.5 mm were produced using the Bioscaffolder® device (Sys-Eng, Germany). The scaffolds were designed in Inventor while PrimCam (Sys-Eng, Germany) was used to create the final structure. The needle was a gauge 27, the pressure was maintained at 5 bar and the temperature was set to 120 °C. The selected lay-down pattern was 0/90 ° and the anticipated pore size was 300 µm.[26,27]

Scaffold surface modification

Oxygen plasma modification

Scaffolds were subjected to an oxygen plasma treatment (dielectrical discharge plasma reactor, Model Femto, version 3, Diener Electronic, Germany) for 60 s.[27] These scaffolds will be denoted as PCL O.

Multi-step gelatin-fibronectin modification

Scaffolds were subjected to a multi-step procedure involving a double protein coating of gelatin and fibronectin.[24-26] Briefly, PCL scaffolds were pre-activated by Ar plasma treatment followed by exposure to the atmosphere. These scaffolds were immersed in a 1M AEMA solution and subsequently subjected to UV-irradiation. After thoroughly rinsing with deionised water, the scaffolds were immersed in 1 mg/ml gelatin type B (gelB) solution in distilled water. Subsequently, 1 mg/ml water soluble 1-ethyl-3(-3-dimethylaminopropyl) carbodiimide hydrochloride solution was added. After this immobilization step, several cleaning cycles were performed using deionised water followed by an overnight incubation at 37 °C. In the last modification step, the scaffolds were coated with Fn by immersion in 0.1

mg/ml Fn solution for 60 s followed by drying at ambient atmosphere. These scaffolds will be denoted as PCL Fn.

PCL O and PCL Fn scaffolds were sterilized using ethylene oxide (UZGhent) for the cell culture experiments.

Reference scaffolds

BD™ three dimensional OPLA® scaffolds (LA O) (Cat. No. 354614) and BD™ three dimensional Collagen scaffolds (COL) (Cat. No. 354613) (Becton Dickinson (Erembodegem, Belgi ë)) were used as reference materials. LA O is synthesized from D,D-L,L polylactic acid and oxidized by an atmospheric plasma treatment. COL is comprised of a mixture of soluble and fibrillar collagen (type I and type II collagens). These sponge-type 3D reference scaffolds have a diameter of 4.7 mm and a height of 2.25 mm.

Scaffold characterization

SEM analysis was performed on a JEOL JSM-5600 (JEOL, Japan) instrument. The apparatus was used in the secondary electron mode (SEI). Different dimensions of the scaffold were measured: strut diameter, interstrut distance, height of the struts and pore size (mean and SD of triplicate values). The porosity of 3D plotted scaffolds was calculated.[28] Bioplotted PCL and the conventional scaffolds were evaluated using inverted contrast light microscopy (Olympus inverted Research System Microscope, Cell^M software, Olympus, Belgium).

Cell culture and cell seeding onto PCL and conventional scaffolds

ADSC (Cryo-Save, Belgium) were plated at a density of 5000 cells/cm^2 in MesenPRO (Invitrogen) and expanded until P3-6 that were used for all experiments performed in our study. Cells were cultured at 37 ℃ (5% CO_2). For the cell/scaffold experiments, cells were

cultured in α-MEM glutamax (Gibco Invitrogen) supplemented with 10% foetal calf serum (FCS, Gibco Invitrogen) and 0.5 vol% penicillin-streptomycin (10,000 U/ml-10,000 µg/ml, Gibco Invitrogen) named as standard medium.

Before cell seeding, the scaffolds were immersed in serum-free standard medium in Eppendorf tubes. Air was removed from their pores by generating vacuum with a 20 ml syringe equipped with a gauge 18 needle. The scaffolds were left in medium on a gyratory shaker (37 ℃, 70 rpm). After 24 h, the scaffolds were placed into 96-well tissue culture dishes (for suspension culture). Cells were seeded at a density of 0.75 x 10^6 cells/40 µl/scaffold and were allowed to adhere for 4 hours. Medium (160 µl) was added to each well and the seeded scaffolds were further incubated overnight. After 24 h, cell/scaffold constructs were placed in a 12 well plate. Three ml osteogenic culture medium (standard medium supplemented with 100 µM L-ascorbic acid 2-phosphate (Sigma), 100 nM dexamethasone (Sigma) and 10 mM β-glycerophosphate (Sigma)) was added and the cell/scaffold constructs were cultured for 28 days (5% CO_2/95% air, 37 ℃) with a culture medium change twice a week.

Characterization of cell/scaffold constructs

Cell seeding efficiency, adhesion, proliferation, colonization and differentiation were evaluated at different time points (1, 7, 14 and 28 days post-seeding).

Seeding efficiency

12 hours post-seeding, the scaffolds were removed and the remaining cells in the wells were counted using a counting chamber. The seeding efficiency was calculated using the equation:

seeding efficiency (%) = (cells added to scaffold – residual cells in well)/cells added to scaffold x 100. (Mean and SD of 12 replicates).

Phase contrast and fluorescence microscopy

To visualize cell adhesion and colonization on the scaffolds, cell/scaffold constructs were evaluated using inverted contrast light microscopy and fluorescence microscopy (Olympus

inverted Research System Microscope, type U-RFL-T, Cell^{M} software, Olympus, Belgium) after calcein AM/propidium iodide staining as described previously.[21]

Histology

Cell/scaffold constructs were rinsed with PBS, fixed with 4% phosphate (10 mM) buffered formaldehyde (pH 6,9) (4 ℃, 24 h), dehydrated and embedded in paraffin. 5-7 µm sections were stained with hematoxylin & eosin (H&E) and Masson's Trichrome and mounted with mounting medium (Cat.No. 4111E, Richard-Allan Scientific).

Immunohistochemistry

Immunohistochemistry, using antibodies (Ab) directed against, collagen I (polyclonal rabbit anti-human, Acris R1038, Acris) and osteocalcin (polyclonal goat anti-human, V-19 sc-18319, Santa Cruz Biotechnology) was performed on the tissue sections as described previously.[21]

Protein assay and alkaline phosphatase activity

Cell/scaffold constructs were lysed into 0.5 ml of a 1% Triton X-100 containing Tris HCl buffer, homogenized by two freeze-and-thaw cycles and sonicated on ice for 3 x 10 s (amplitude of 40 %) (Vibra Cell^{TM} SONICS (ANALIS)). Protein content and alkaline phosphatase (ALP) were determined as previously.[29] ALP activity was expressed as mM p-nitrophenol/mg protein.

Real-time RT-PCR analysis

ADSC cultures were trypsinized, collected and centrifuged at 1000 rpm, 5 min. After removal of the supernatant, TRI Reagent was added. Cell/scaffold constructs were rinsed in PBS and TRI Reagent was added. RNA was isolated followed by DNA treatment and RNA was transcribed to cDNA. Real time PCR was performed on the ABI 7500 Fast Real Time PCR device with Taqman probes for the following genes: runt-related transcription factor (Runx2), collagen type I (COL1A1) and osteocalcin (OCN) as described previously.[21] Relative quantification (Rq, n fold expression) values were calculated using the equation $2^{-\Delta\Delta Ct}$.

Statistical analysis

A Mann-Whitney test using SPSS 19.0 was performed to compare the differences among groups. Differences among groups were considered as statistically significant when $p \leq 0.05$. Mean and SD were reported in each Fig.

RESULTS

Scaffold characterization

In Fig. 1, a photograph of the Bioscaffolder® (a) and a plotted PCL scaffold with a 0/90 lay-down pattern (a, insert) are presented. SEM-images of a top-view (c) and a cross-section (d) are presented. The scaffold properties are presented in Table 1, according to the scaffold dimensional parameters (Fig. 1 b). Phase-contrast micrographs of the scaffolds are shown in Fig. 2. The plotted scaffolds (Fig. 2 (a, d)) consist of repeating structural units, well controlled interconnected pores with a pore size of ± 300 µm and a porosity of 60-78%. This is in contrast to LA O (Fig. 2 (b, e)) and COL (Fig. 2 (c, f)) scaffolds, which have a more compact architecture, an irregular structure and pore morphology (pore size ± 100-200 µm) and a porosity of 90-98 %. The fibrillar network of both scaffolds is presented in Fig. 2 (c, f).

The characterization of surface modified PCL scaffolds by direct oxygen plasma (PCL O) and a multistep procedure involving post-argon plasma AEMA grafting, gelB immobilization and Fn physisorption (PCL Fn) was reported earlier.[24,25,27,30]

Cell seeding efficiency

The seeding efficiency is presented in Fig. 3 a. Low seeding efficiencies were obtained for plotted PCL scaffolds: PCL O (45.1 ± 15.9 %) and PCL Fn (33.3 ± 8.1 %). Conventional LA

O and COL based scaffolds reach seeding efficiencies of 78.6 ± 2.6 % respectively 82.7 ± 5.5 %.

Cell proliferation and colonization

The results of cell imaging for plotted and conventional scaffolds as a function of time is depicted in Fig. 4. After 4 hours, a lot of round, non-adherent cells between the polymer struts of the plotted scaffolds are visible by phase-contrast microscopy (Fig. 4 a, a', b, b'). Round cells can also be detected on the conventional scaffolds (Fig. 4 c, c', d, d'). After 7 days, the polymer struts of the plotted scaffolds are completely covered with viable cells, independent of the surface modification (Fig. 4 e, f). The cells are bridging the pores of the plotted scaffolds (elongated cells) (Fig. 4 e', f'). The surface of LA O and COL is completely covered with viable cells (Fig. 4 g, h). After 14 days, the surface of the plotted scaffolds is completely covered with viable cells and bridging of the pores continues (Fig. 4 i, i', j, j'). The cellular appearance and the amount of viable cells on the surface of the conventional scaffolds remains unchanged (Fig. 4 k, k', l).

In a next step, we were interested to study cellular colonization in the scaffolds by looking at cross-sections as shown in Fig. 5. After 7 days, PCL O scaffolds are colonized only at the edge of the scaffold. In the center of the scaffold, no cells are present (Fig. 5 a). PCL Fn scaffolds show a better colonization in the center of the scaffold. The pores are completely filled with cellular material (Fig. 5 b). The LA O and COL scaffolds show only cell layers at the edges of the scaffolds (Fig. 5 c, d). After 28 days in culture, the colonization of PCL O scaffolds is still limited mostly to the edge of the scaffold (Fig. 5 e'). In the center of the scaffold, almost no colonization is detected (Fig. 5 e). In contrast, plotted PCL Fn scaffolds are homogeneously colonized throughout the scaffold (Fig. 5 f). This is in contrast to the conventional scaffolds where the cellular colonization did not proceed towards the center of

the scaffold (Fig. 5 g, h). More cell layers can be observed in COL (Fig. 5 h) than LA O (Fig. 5 g) scaffolds.

The protein content of cell/scaffold constructs after 28 days is shown in Fig. 3 b. The protein content is highest for COL followed by PCL Fn, LA O and PCL O. The protein content of blanc protein-based scaffolds (PCL Fn and COL) was negligible. Oxidized (PCL O and LA O) respectively protein-based scaffolds (PCL Fn and COL) have a comparable proliferation ratio (Fig. 3 b).

Extracellular matrix formation

The ECM formation is visualized in Fig. 6. After 7 days, a dense layer of cells can be seen on the periphery of LA O (Fig. 6 c) and COL (Fig. 6 d) scaffolds. The initial ECM formed at the edge of the conventional scaffolds already has a dense appearance. In contrast, plotted PCL scaffolds are colonized at the edge (PCL O) or throughout the scaffold (PCL Fn) (Fig. 6 a, b). For both plotted scaffolds, the ECM formation is loose (Fig. 6 e, f). For PCL Fn scaffolds, the ECM is uniformly distributed throughout the scaffold (Fig. 6 b, f).

After 28 days, the ECM remains loose in the plotted scaffolds (Fig. 6 i, j, m, n). Sometimes, a more dense ECM can be observed at the edge (Fig. 6 n') or between the narrow space of 2 struts (artefact) (Fig. 6 m'). In the conventional scaffolds, the ECM is dense and situated parallel to the surface of the scaffold (Fig. 6 k, l, o, p). In the center, almost no ECM can be observed.

Differentiation

In a last part of our work, we assessed cell differentiation by evaluating the levels of ALP; Runx2, COL1α1, OCN phenotypic expression and (immuno) histochemistry.

ALP was undetectable for the plotted scaffolds after 7 days, compared to the conventional scaffolds. However, after 14 and 28 days, the ALP activity has increased drastically for these structures and reaches similar values as the conventional scaffolds (Fig. 7 a). The phenotypic expression of Runx2 is upregulated after 7 days in COL and PCL Fn scaffolds. An upregulation of COL1α1 can be observed for the PCL Fn scaffold. An upregulation of OCN can already be noticed for the COL scaffold. For all plasma treated scaffolds (PCL O and LA O), the three osteogenic markers are down regulated. After 14 days, Runx2 is upregulated for all the scaffolds except LA O. Also COL1α1 is upregulated in all scaffolds, but highest for PCL Fn and COL. Also OCN is upregulated in all scaffolds, but highest in the protein-based scaffolds (PCL Fn and COL). After 28 days, COL1α1 is still upregulated in protein-based scaffolds (PCL Fn and COL). OCN upregulation is more pronounced in PCL Fn, followed by PCL O, COL and LA O (Fig. 7 d).

Immunohistochemical analysis of the osteogenic differentiation of ADSCs in plotted PCL compared with conventional scaffolds is presented in Fig. 8. The formation of an ECM by ADSC after 28 days in culture was observed in both plotted and conventional scaffolds. However, it must be noted that the conventional scaffolds (LA O and COL) show an intense staining of ECM by Trichrome Masson (Fig. 8 c, d, g, h) in contrast to plotted scaffolds where the stain is less intense (Fig. 8 a, b, e, f). Only at the edge (Fig. 8 f') or between the narrow space of 2 artefact struts, the ECM is stained more intense (Fig. 8 e'). The ECM is staining positive for collagen I. Collagen I was observed predominantly at the periphery of the conventional scaffolds (Fig. 8 k, l) and almost throughout the plotted scaffolds (Fig. 8 i, j). Again the collagen I immunostaining is more intense on the conventional than plotted scaffolds. Also OCN can be detected in both plotted and conventional scaffolds. The ECM of plotted scaffolds stains less intense for OCN than the conventional scaffolds. It must be

reported that OCN already could be detected by immunostaining after 7 days (photograph not shown), which was also detected by qRT-PCR.

DISCUSSION

In TE, the scaffold plays an important role as temporary support for the development of new tissue either through *in vivo* cell invasion or through *in vitro* culturing cells on the scaffold prior to implantation. In this regard, tissue formation in 3D scaffolds is influenced by the scaffold design and composition. Hence, the architecture and physico-chemical properties of the scaffold that support cell colonization, growth and differentiation need to be considered. Scaffold architecture influences passive cell distribution while seeding as well as active cell movement and tissue formation.[4] The scaffold composition should elicit certain biological cues to direct the cells towards colonization and tissue formation.

In the present study, we analyzed the influence of scaffold architecture and composition on mesenchymal stem cell adhesion, colonization and differentiation. Two bioplotted PCL scaffolds (surface modified with respectively an oxygen plasma and a gelatin/fibronectin coating) with an open pore and uniform structure were compared with more compacted, irregular oxidized polylactic acid and collagen based scaffolds.

The seeding efficiency has been associated with the surface area available for cells to attach to and the surface characteristics influencing the ability of cells to adhere. In addition, also the scaffold architecture and pore structure could play an important role.[31]

In our study, no increase in seeding efficiency of double protein coated PCL (PCL Fn) compared with plasma modification of PCL scaffolds (PCL O) was found. Also the conventional plasma treated LA (LA O) scaffold had a comparable seeding efficiency as the COL scaffold. Cell seeding onto plotted PCL scaffolds was significantly lower (39.2 $\pm$ 8.3 %)

compared to the conventional scaffolds (81.9 ± 1.0 %). The two scaffold types (plotted versus conventional scaffolds) on which cells were seeded on the surface clearly showed the effect of scaffold architecture. The conventional scaffolds (COL and LA O) are the densest and retain the cells on the surface. In contrast, plotted scaffolds have an open pore network and are highly geometrical leading to cell loss during seeding. The biomimetic surface modification of the 3D PCL plotted scaffold did not contribute to a higher cell seeding efficiency. Consistent with other studies, higher seeding efficiencies were reported for more compacted architectures.[10,31,32] From these results, we can suggest that 3D scaffold architecture has a more profound influence on the seeding efficiency than surface chemistry, at least with the pore size geometry combination evaluated in the present work.

Although a biomimetic coating (PCL Fn) or scaffold (COL) did not increase the seeding efficiency compared to oxidized scaffolds (PCL O and LA O), protein-based surfaces (PCL Fn and COL) did have a clear benefit on the proliferation and colonization of ADSC. PCL O and LA O showed little proliferation, whereas PCL Fn and COL showed a high increase in cell/protein content. Histology demonstrated that only the edges of the PCL O scaffolds were colonized, but not the center of the scaffolds, while for PCL Fn the complete structure was colonized after 28 days. COL and LA O scaffolds were only colonized at the edges, but the peripheral tissue layer was more dense on COL scaffolds.

We can thus conclude that both surface modification and scaffold architecture have a clear influence on the cellular proliferation and colonization. The influence of a protein-based surface modification was also reported by Yildirim *et al.* who observed an increased cell amount in an oxygen plasma/Fn modification of PCL compared to plasma-only modified PCL.[14] Consistent with other reports[4,33,34], a limited colonization at the edge of the conventional scaffolds was observed resulting in a strong gradient of cell density from the surface to the inner scaffold region.

As tissue formation is often preceded by high cell densities, the observed difference in seeding efficiency, proliferation and colonization between the scaffolds, varying in architecture and composition, will inevitally lead to differences in ECM formation and differentiation. In conventional scaffolds (LA O and COL) with a compact design, a dense ECM is formed at the edge of the scaffold already after 7 days in culture. In contrast, the ECM formed in plotted scaffolds was loose even after 28 days in culture. This is reflected in the osteogenic differentiation: ALP activity and late-stage osteogenic markers (OCN) in conventional scaffolds could already be detected after 1 week. Kumar *et al*. described that scaffold structure was more influential than scaffold composition on the cellular gene expression of human bone marrow stromal cells.[35] Nevertheless, during further culture periods, the osteogenic markers in plotted scaffolds reached levels competing with the conventional scaffolds. Cells on protein based surfaces (PCL Fn and COL) did show increased osteogenic marker expression throughout the whole culture period. Also Yildirim *et al*. reported that a combined plasma/Fn modified scaffold leaded to a higher ALP activity compared to plasma-only modified scaffolds.[14] In general, it can be concluded that protein-based surfaces stimulate the differentiation of ADSC towards bone cells. However, it should be noticed that the cell differentiation on uniform, open pore structured scaffolds produced by RP is delayed compared to the differentiation on compact, irregular pore structured scaffolds processed by conventional techniques. It can be hypothesized that this is due to the fact that cells need a longer proliferation period on the plotted scaffolds, in order to colonize the complete structure. Therefore, the required cell density to differentiate is reached at a later stage compared to the conventional scaffolds where the cells remain on the edge. Cipitria *et al*. reported that plotted scaffolds acted as a guiding substrate to enable the formation of a fibrous network as a prerequirement for later bone formation. The fibrous network morphology, which in turn is guided by the scaffold architecture, influences the

microstructure of the newly formed bone. A structured fibrous tissue across the entire defect was formed, which acted as a secondary supporting network for cells.[36]

The double protein modified PCL scaffold, combining the advantages of the bioplotter technology and the biomimetic properties, is a promising scaffold serving as a guiding template during the bone regeneration process. Future directions in guided tissue regeneration will focus on optimalization of scaffold design by tailoring the scaffold structure or by combining multiple processing techniques to create hybrid scaffolds.[35,37,38]

CONCLUSIONS

In the present study, PCL scaffolds were plotted applying the 3D Bioscaffolder® technology and successfully modified with two surface modification strategies: an oxygen plasma modification and a double protein biomimetic coating. Uniform but loose tissue formation was obtained in both plotted scaffolds in contrast to conventional scaffolds, where the tissue formation is dense but non-homogeneous. The biomimetic coating of PCL resulted in an increased osteogenic differentiation compared with oxygen plasma-only modified PCL scaffolds, but a delayed differentiation compared with scaffolds with a more compact architecture. In conclusion, the present study successfully demonstrates that biomimetic PCL scaffolds can serve as a guiding template to obtain a uniform bone tissue formation.

ACKNOWLEDGEMENTS

The authors would like to thank David Schaubroeck for the SEM images. A special thanks to Leen Pieters and Toke Thiron for the excellent technical assistance. This work was supported by the FWO research grant G.0006.10 and the Ghent University by providing Dr. H. Declercq a postdoc mandate (BOF IV1-I/0002/03).

AUTHOR DISCLOSURE STATEMENT

No competing financial interests exist.

REFERENCES

1. Kierszenbaum, A.L. In Histology and Cell Biology. An introduction to pathology, pp. 131-133. St. Louis: Mosby. 2002

2. Wang, H., and van Blitterswijk, C. A. The role of three-dimensional polymeric scaffold configuration on the uniformity of connective tissue formation by adipose stromal cells. Biomaterials **31**, 4322, 2010.
3. Kim, K., Dean, D., Wallace, J., Breithaupt, R., Mikos, A. G., and Fisher, J. P. The influence of stereolithographic scaffold architecture and composition on osteogenic signal expression with rat bone marrow stromal cells. Biomaterials **32**, 3750, 2011.
4. Nuernberger, S., Cyran, N., Albrecht, C., Redl, H., Vécsei, V., and Marlovits, S. The influence of scaffold architecture on chondrocyte distribution and behavior in matrix-associated chondrocyte transplantation grafts. Biomaterials **32**, 1032, 2011
5. Moroni, L., de Wijn, J. R., and van Blitterswijk, C. A. 3D fiber-deposited scaffolds for tissue engineering: influence of pores geometry and architecture on dynamic mechanical properties. Biomaterials **27**, 974, 2006.
6. Woodruff, M. A., and Hutmacher, D. W. The return of a forgotten polymer-polycaprolactone in the 21st century. Prog Polym Sci **35**, 1217, 2002.
7. Seyednejad, H., Gawlitta, D., Dhert, W. J. A., van Nostrum, C. F., Vermonden, T., and Hennink, W. E. Preparation and characterization of a three-dimensional printed scaffold based on a functionalized polyester for bone tissue engineering applications. Acta Biomater **7**, 1999, 2011.
8. Cheng, Z. Y., and Teoh, S. H. Surface modification of ultra thin poly (epsilon-caprolactone) films using acrylic acid and collagen. Biomaterials **25**, 1991, 2004.
9. Hoque, E., San, W. Y., Wei, F., Li, S., Huang, M. H., Vert, M., and Hutmacher, D. W. Processing of polycaprolactone and polycaprolactone-based copolymers into 3D scaffolds, and their cellular responses. Tissue Eng **15**, 3013, 2009.

10. Park, S. A., Lee, S. H., and Kim, W.D. Fabrication of porous polycaprolactone/hydroxyapatite (PCL/HA) blend scaffolds using a 3D plotting system for bone tissue engineering. Bioproc Biosyst Eng **24**, 505, 2011.
11. Lee, H., and Kim, G. Three-dimensional plotted PCL/β-TCP scaffolds coated with a collagen layer: preparation, physical properties and *in vitro* evaluation of bone tissue regeneration. J Mater Chem **21**, 6305, 2011.
12. Oliveira, A. L., Costa, S. A., Sousa, S. A., and Reis, R. L. Nucleation and growth of biomimetic apatite layers on 3D plotted biodegradable polymeric scaffolds: effect of static and dynamic coating conditions. Acta Biomater **5**, 1626, 2009.
13. Chim, H., Hutmacher, D.W., Chou, A.M., Oliveira, A.L., Reis, R.L., Lim, T. C., and Schantz, J.T. A comparative analysis of scaffold material modifications for load-bearing applications in bone tissue engineering. Int J Oral Max Surg **35**, 928, 2006.
14. Yildirim, E. D., Pappas, D., Güçeri, S., and Sun, W. Enhanced cellular functions on polycaprolactone tissue scaffolds by O2 plasma surface modification. Plasma Process Polym **8**, 256, 2011.
15. Park, S. A., Lee, S. H., Kim, W., Han, I., and Park, J. C. Effect of plasma treatment on scaffold by solid freeform fabrication. J Tissue Eng Regen Med **8**, 23, 2011.
16. Yildirim, E. D., Besunder, R., Pappas, D., Allen, F., Güçeri, S., and Sun, W. Accelerated differentiation of osteoblast cells on polycaprolactone scaffolds driven by a combined effect of protein coating and plasma modification. Biofabrication **2**, 1, 2010.
17. Zhang, H., Lin, C. Y., and Hollister, S.J. The interaction between bone marrow stromal cells and RGD-modified three-dimensional porous polycaprolactone scaffolds. Biomaterials **30**, 4063, 2009.

18. Siow, K. S., Britcher, L., Kumar, S., and Griesser, H.J. Plasma methods for the generation of chemically reactive surfaces for biomolecule immobilization and cell colonization- a review. Plasma Process Polym **3**, 392**,** 2006.

19. Chu, P. K., Chen, J. Y., Wang, L. P, and Huang, N. Plasma-surface modification of biomaterials. Mater Sci Eng R **36**, 143, 2002.

20. Desmet, T., Morent, R., De Geyter, N., Leys, C., Schacht, E., and Dubruel, P. Nonthermal plasma technology as a versatile strategy for polymeric biomaterials surface modification: a review. Biomacromolecules **10**, 2351, 2009.

21. Declercq, H. A., De Caluwé, T., Krysko, O., Bachert, C., and Cornelissen, M.J. Bone grafts engineered from human adipose-derived stem cells in dynamic 3D-environments. Biomaterials **34**, 1004, 2013.

22. Ferreira, A. M., Gentile, P., Chiono, V., and Ciardelli, G. Collagen for bone tissue regeneration. Acta Biomater **8**, 3191, 2012.

23. Van Vlierberghe, S., Vanderleyden, E., Dubruel, P., De Vos, F., and Schacht, E. Affinity study of novel gelatin cell carriers for fibronectin. Macromol Biosci **9**, 1105, 2009.

24. Desmet, T., Billiet, T., Berneel, E., Cornelissen, R., Schaubroeck, D., Schacht, E., and Dubruel, P. Post-plasma grafting of AEMA as a versatile tool to biofunctionalise polyesters for tissue engineering. Macromol Biosci **10**, 1484, 2010.

25. Desmet, T., Poleunis, C., Delcorte, A., and Dubruel, P. Double protein functionalized poly-ε-caprolactone surfaces: in depth ToF-SIMS and XPS characterization. J Mater Sci-Mater M **23**, 293, 2012.

26. Berneel, E., Desmet, T., Declercq, H., Dubruel, P., and Cornelissen, M. Double protein-coated poly-ε-caprolactone scaffolds: succesful 2D to 3D transfer. J Biomed Mater Res A **100A**, 1783, 2012.

27. Desmet, T., Billiet, T., Berneel, E., Cornelissen, M., and Schacht, E. The effect of plasma treatment on the properties of 3D, biodegradable cell substrates developed using rapid prototyping technology. Workshop Engineering of Functional Interfaces, **101**, 2009.

28. Landers, R., Pfister, A., Hübner, U., John, H., Schmelziesen, R., and Mülhaupt, R. Fabrication of soft tissue engineering scaffolds by means of rapid prototyping techniques. J Mater Sci **37**, 3107, 2002.

29. Declercq, H., Van den Vreken, N., De Maeyer, E., Verbeeck, R., Schacht, E. De Ridder, L., and Cornelissen, M. Isolation, proliferation and differentiation of osteoblastic cells to study cell/biomaterial interactions: comparison of different isolation techniques and source. Biomaterials **25**, 757, 2004.

30. Kersemans, K., Desmet, T., Vanhove, C., Dubruel, P., and De Vos, F. Radiolabeled gelatin type B analogues can be used for non-invasive visualization and quantification of protein coatings on 3D porous implants. J Mater Sci-Mater M **23**, 1961, 2012.

31. Sobral, J. M., Caridade, S. G., Sousa, R. A., Mano, J. F., and Reis, R. L. Three-dimensional plotted scaffolds with controlled pore size gradients: effect of scaffold geometry on mechanical performance and cell seeding efficiency. Acta Biomater **7**, 1009, 2011.

32. Yilgor, P., Sousa, R. A., Reis, R. L., Hasirci, N., and Hasirci, V. 3D plotted PCL scaffolds for stem cell based bone tissue engineering. Macromol Symp **269**, 92, 2008.

33. Murphy, C. M., Haugh, M. G., and O' Brien, F. J. The effect of mean pore size on cell attachment, proliferation and migration in collagen-glycosaminoglycan scaffolds for bone tissue engineering. Biomaterials **31**, 461, 2010.

34. Lyons, F. G., Al-Munajjed, A. A., Kieran, S. M., Toner, M. E., Murphy, C. M., Duffy, G.P., and O'Brien, F.J. The healing of bony defects by cell-free collagen-based scaffolds compared to stem cell-seeded tissue engineered constructs. Biomaterials **31**, 9232, 2010.

35. Kumar, G., Tison, C. K., Chatterjee, K., Pine, P. S., McDaniel, J. H., Salit, M. L., Young, M. F., and Simon, C. G. The determination of stem cell fate by 3D scaffold structures through the control of cell shape. Biomaterials **32**, 9188, 2011.

36. Cipitria, A., Lange, C., Schell, H., Wagermeier, W., Reichert, J.C., Hutmacher, D.W., Fratzl, P., and Duda, G.N. Porous scaffold architecture guides tissue formation. J Bone Mineral Res **27**, 1275, 2012.

37. Moroni, L., Schotel, R., Hamann, D., de Wijn, J. R., and van Blitterswijk, C. A. 3D fiber-deposited electrospun integrated scaffolds enhance cartilage tissue formation. Adv Funct Mater **18** ,53, 2008.

38. Yeo, M., Lee, H., and Kim, G. Three-dimensional hierarchical composite scaffolds consisting of polycaprolactone, β-tricalcium phosphate, and collagen nanofibers: fabrication, physical properties, and in vitro cell activity for bone tissue regeneration. Biomacromolecules **12**, 502, 2011.

Address correspondence to:

Maria Cornelissen, PhD

Department of Basic Medical Sciences

Ghent University

De Pintelaan 185 (6B3)

9000 Ghent

Belgium

E-mail: ria.cornelissen@ugent.be

FIGURE LEGENDS

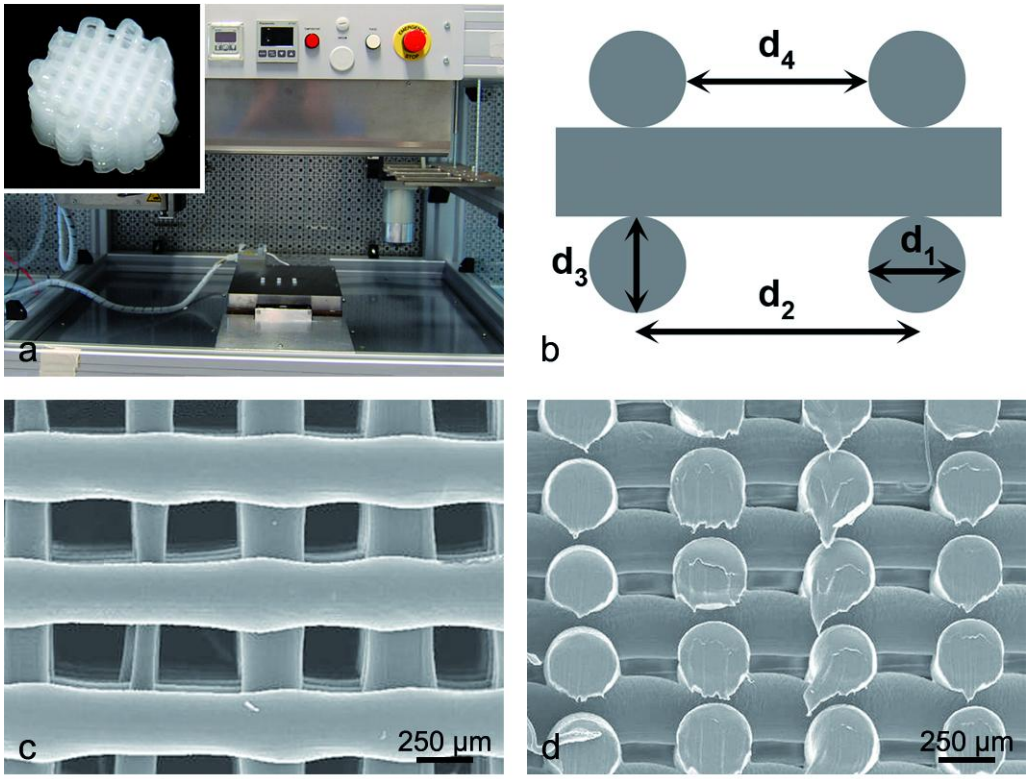

Fig. 1.

Fig. 1. Fabrication and characterization of bioplotted PCL scaffolds. a) Bioscaffolder® device, a insert) photograph of a bioplotted PCL scaffold, b) bioplotted scaffold dimensional parameters. d_1: fiber diameter, d_2:interstrut distance, d_3: layer thickness, d_4: pore size, c-d) SEM images (top-view and cross-section).

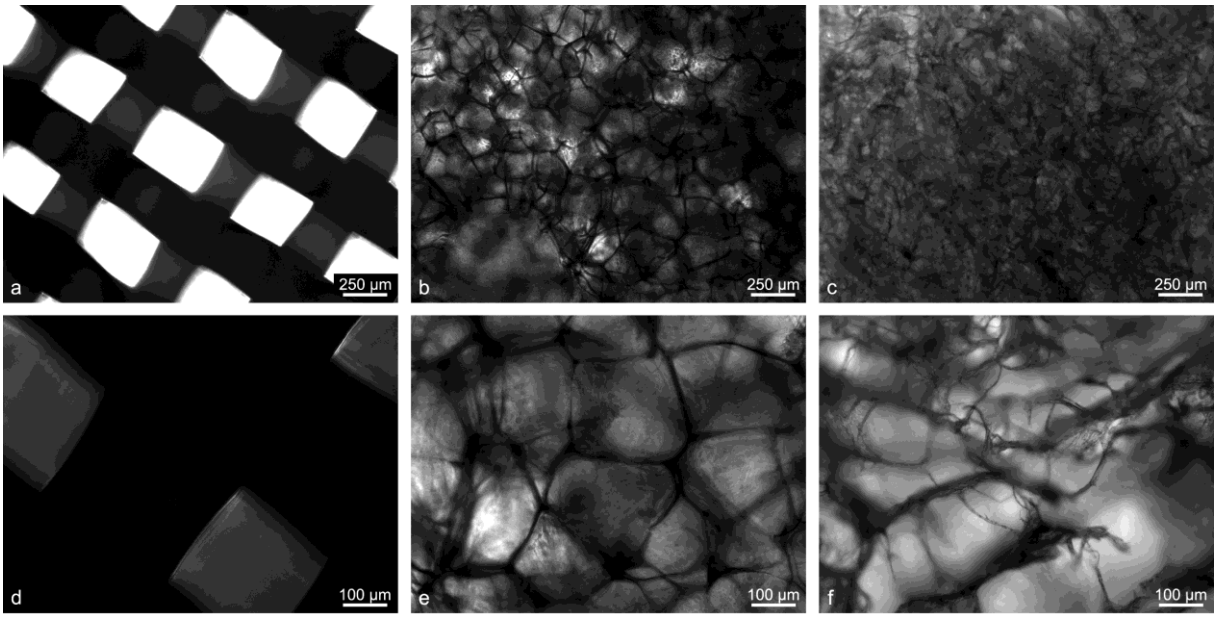

Fig. 2.

Fig. 2. Phase-contrast images. a, d) PCL scaffold (0/90 ° pattern), b, e) LA O scaffold, c, f) COL scaffold.

Table 1.

Scaffold	Interstrut d_1 (µm)	Interstrut d_2 (µm)	Interstrut d_3 (µm)	Pore size (d_4) (µm)	Porosity (%)
PCL 0/90	253 ± 29	593	288 ± 1	310 ± 24	60-78
LA O	n.a.	n.a.	n.a.	100-200	90-98
COL	n.a.	n.a.	n.a.	100-200	90-98

Table 1. Overview of the scaffold characteristics.

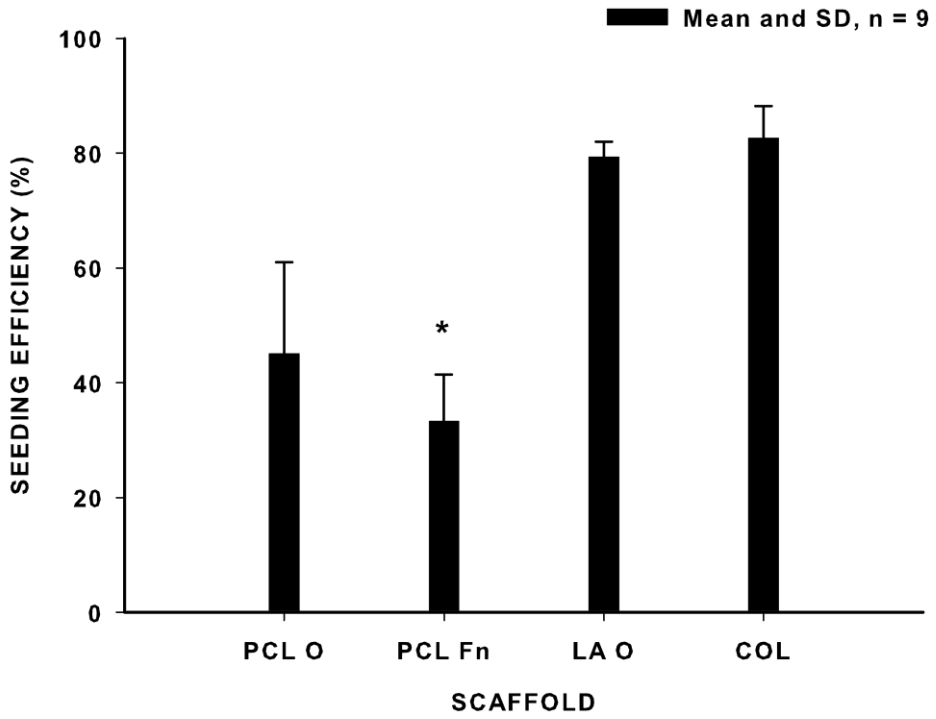

a

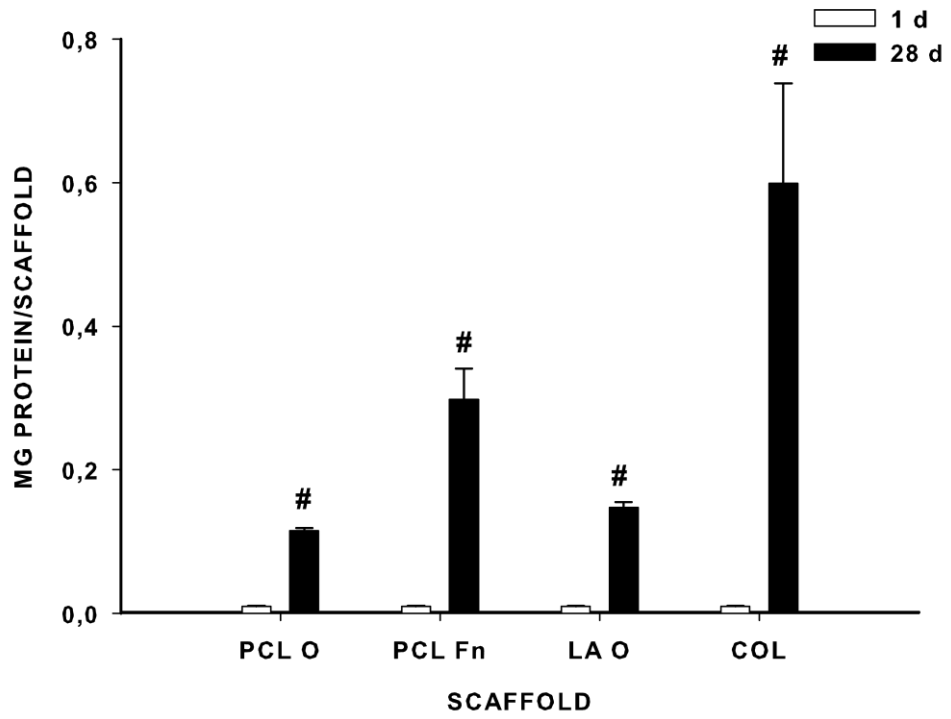

b

Fig. 3.

Fig. 3. a) Seeding efficiency of ADSC on bioplotted (PCL O, PCL Fn) and conventional (LA O, COL) scaffolds. * Statistical difference ($p \leq 0.05$) from LA O and COL. b) Protein content of cell/scaffold constructs cultured in standard medium for 1 and 28 days. # Statistical difference ($p \leq 0.05$) from other groups.

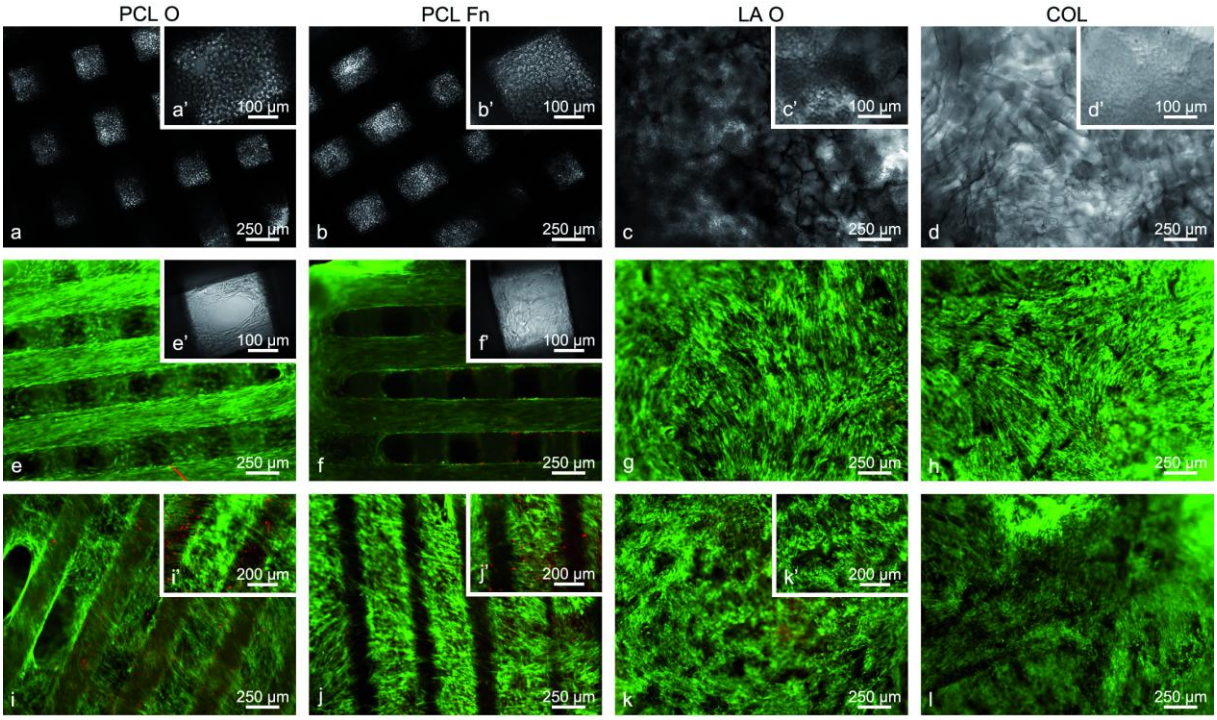

Fig. 4.

Fig. 4. Influence of surface modification and scaffold design on the colonization of the scaffolds. Phase-contrast (a-d, a'-d', e'-f') and fluorescence (e-l, i'-k') (CaAM/PI staining) microscopy of 3D scaffolds after 1 (a-d), 7 (e-h) and 14 (i-l) days in osteogenic medium. a, e, i) PCL O; b, f, j) PCL Fn; c, g, k) LA O and d, h, l) COL.

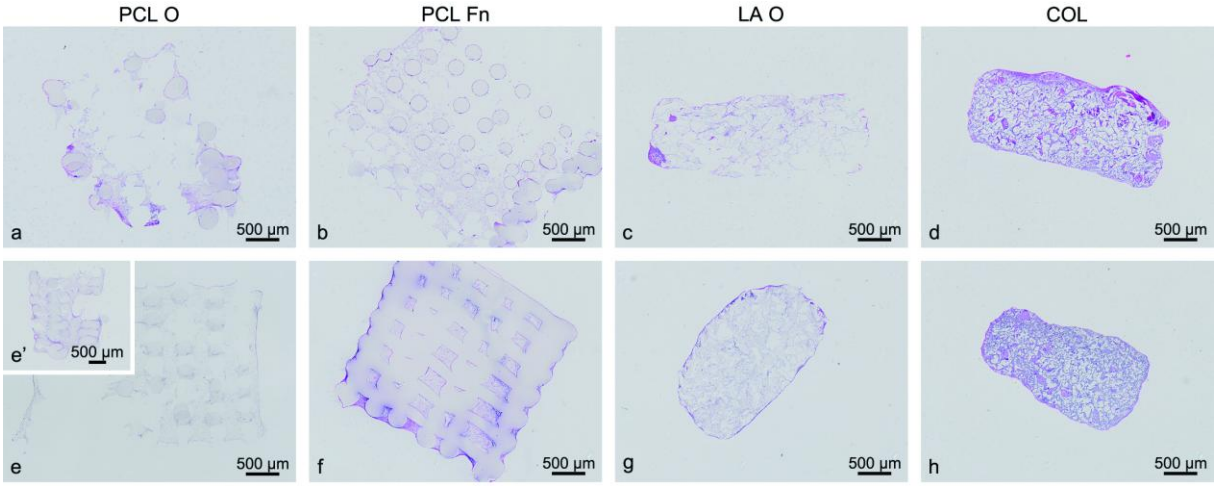

Fig. 5.

Fig. 5. Influence of surface modification and scaffold design on the colonization of the scaffolds. Histological analysis of 3D scaffolds after 7 (a-d) and 28 (e-h) days in osteogenic medium. H& E staining. a, e) PCL O; b, f) PCL Fn; c, g) LA O and d, h) COL.

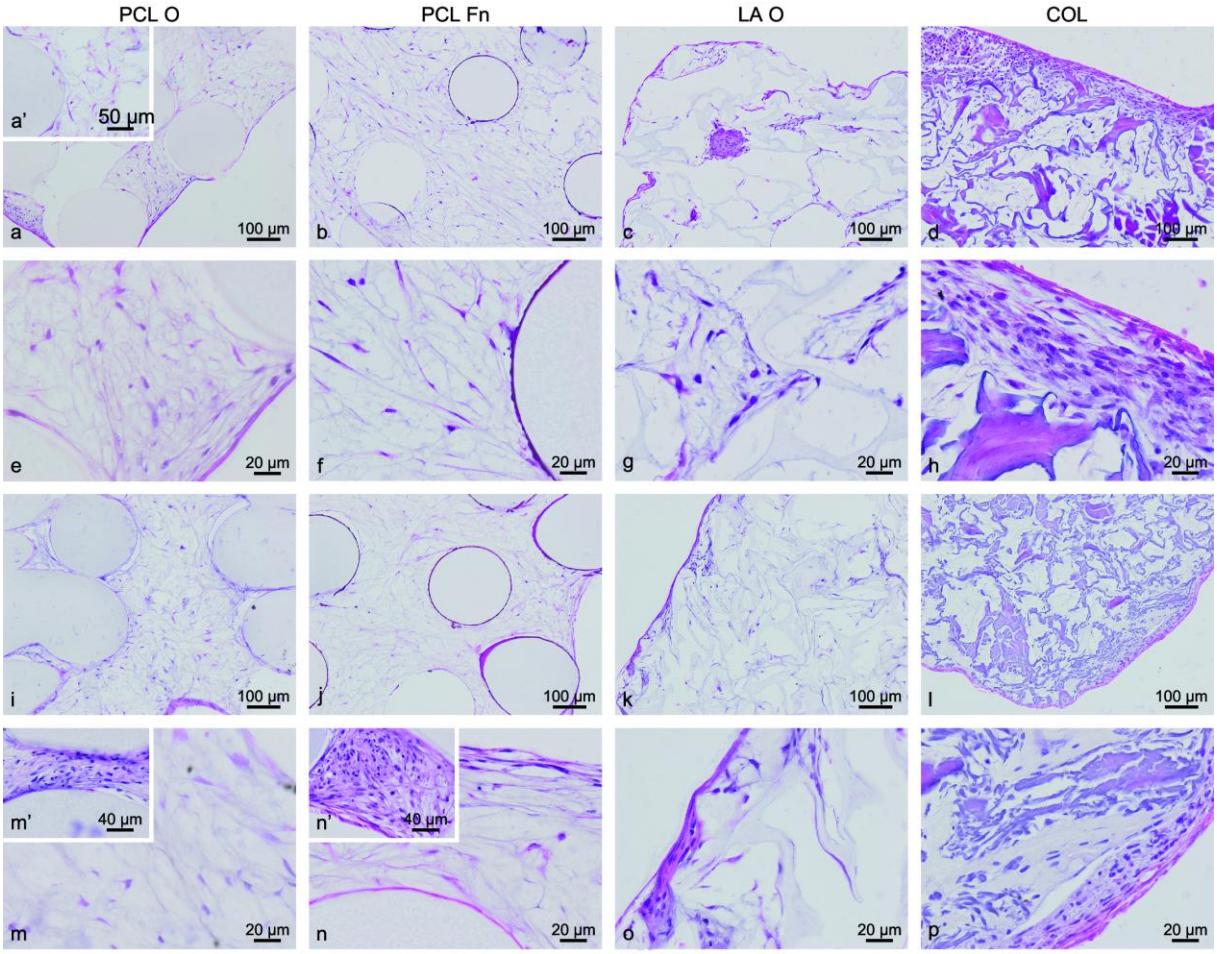

Fig. 6.

Fig. 6. Influence of surface modification and scaffold design on the extracellular matrix formation. Histological analysis of 3D scaffolds after 7 (a-h) and 28 (i-p) days in osteogenic medium. H& E staining. a, e, i, m) PCL O; b, f, j, n) PCL Fn; c, g, k, o) LA O and d, h, l, p) COL.

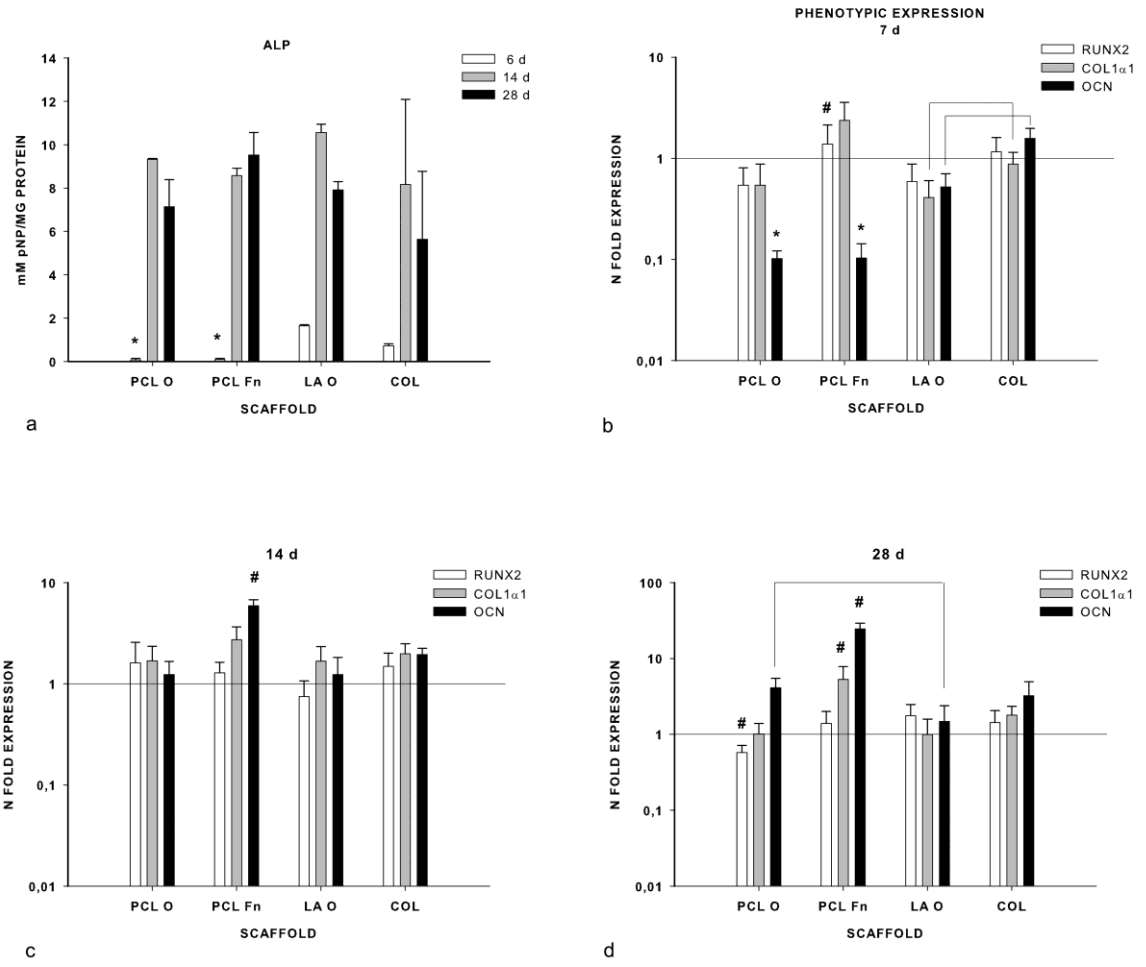

Fig. 7.

Fig. 7. Influence of surface modification and scaffold design on the differentiation of ADSC. a) Alkaline phosphatase activity (mM pNP/mg protein) of ADSC seeded on scaffolds with different surface modification and design after 6, 14 and 28 days. * Statistical difference ($p \leq 0.05$) from LA O and COL. b-d) Gene expression (Runx2, COL1α1, OCN) analysis of ADSC cultured for 7, 14 and 28 days on scaffolds. # Statistical different from other groups. * Statistical different from LA O and COL.

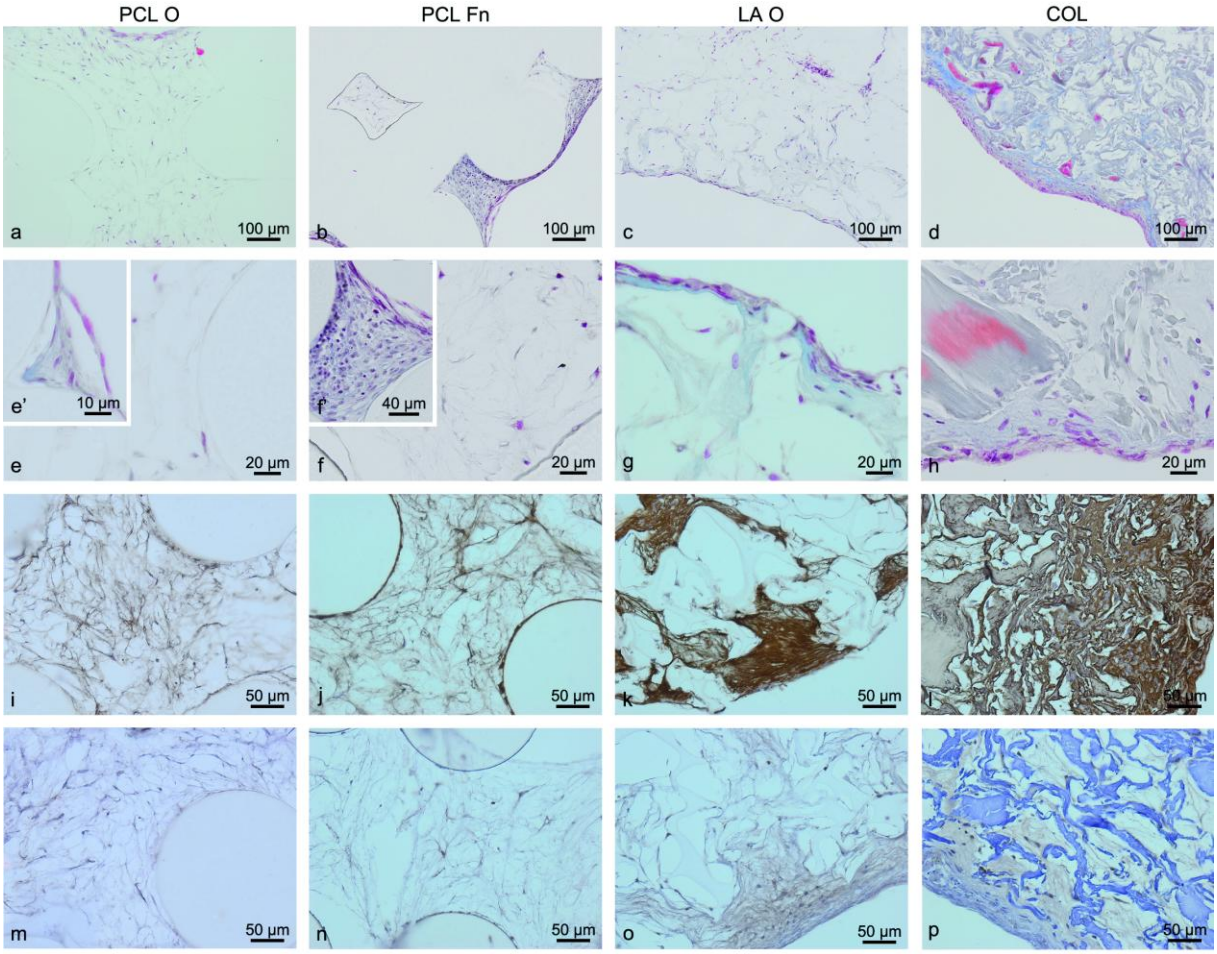

Fig. 8.

Fig. 8. Differentiation of ADSC after 28 days in plotted 3D scaffolds compared with conventional scaffolds. Histological analysis. a, e, i, m) PCL O; b, f, j, n) PCL Fn; c, g, k, o) LA O and d, h, l, p) COL. a-h) Trichrome Masson staining, i-l) collagen I immunostaining and m-p) osteocalcin immunostaining.

Role of scaffold characteristics on bone formation